Efficiently Applicability of Synthetic Cu-TiO₂ in Tetrachloroethene, Trichloroethene and 1,1,1-Trichloroethane Removal in Aqueous Phase under VUV Irradiation

LANDRY BIYOGHE BI NDONG[1], MURIELLE PRIMAELLE IBONDOU[1], XIAOLIANG WU[1],
SHUGUANG LU[1,*], ZHAOFU QIU[1], QIAN SUI[1] and SERGE MAURICE MBADINGA[2]

[1]State Environmental Protection Key Laboratory of Environmental Risk Assessment and Control on Chemical Process, East China University of Science and Technology, Shanghai 200237, P.R. China
[2]State Key Laboratory of Bioreactor Engineering and Institute of Applied Chemistry, East China University of Science and Technology, Shanghai 200237, P.R. China

*Corresponding author: Fax: +86 21 64252737; Tel: +86 21 64250709; E-mail: lvshuguang@ecust.edu.cn; xuminhui@outlook.com

Cu-TiO₂ nano-sheets has been tested by degrading tetrachloroethene, trichloroethene and 1,1,1-trichloroethane in the aqueous phase under VUV illumination. The photo-degradation results revealed the efficient photolysis of these harmful chemicals under VUV irradiation and the addition of synthetic Cu-TiO₂ remarkably enhanced their degradation according to the higher degradation rate observed. Moreover, the fast degradation rate of nitrobenzene, a probe of hydroxyl radicals ($^•$OH), over Cu-TiO₂ suggesting the high concentration of $^•$OH generated in VUV/Cu-TiO₂ system. Cu-TiO₂ has been synthesized by simply hydrothermal solution containing tetrabutyl titanate, hydrofluoric acid and cupric nitrate and characterized by using XRD, BET, TEM and XPS. The characterization results showed that the synthesized doped TiO₂ was in anatase form and consisted of well-defined sheet-shaped structures. It was also showed that the surface state of the synthesized TiO₂ was not modified after Cu doping. It can be suggested that Cu can be used to enhance the photo-catalytic activity of TiO₂ nano-sheets for chlorinated solvent remediation in contaminated groundwater.

Keywords: Cu doping, Titanium dioxide, Chlorinated solvent pollutants, VUV illumination, Groundwater remediation.

INTRODUCTION

Photo-catalysis using semiconductor has been applied as a promising technique for decontamination, purification and/or deodorization of air as well as wastewaters[1-3]. Among worldwide used photo-catalysts, titanium dioxide (TiO₂) is considered to be the most suitable catalyst due to its non-toxicity, biological and chemical inertness, low-cost, strong oxidizing power and the long-term stability against corrosion[4-6]. The drawback is that, a wide band gap energies (3.02 eV) TiO₂ semiconductor needs a long reaction time to completely destroy or transform pollutant into harmless chemicals in both visible and ultraviolet illumination[2,7-9] due to the fast recombination rate of photo-generated electrons and holes. These limitations can be surmounted by treating the surface of the semiconductor such as impurity doping, noble metal deposition and surface fluorination[10-15]. It has also been reported that the crystalline structure, surface area and surface hydroxyl group play key roles in the photo-catalytic activity performance of titanium as in heterogeneous photo-catalysis oxidation reactions usually take place on the surface of semiconductor[16-21]. Choi *et al.*[22]

have conducted a systematic study on the photo-catalytic activity of TiO₂ nanoparticles doped with different transition metals on the oxidation and/or the reduction of CCl₄ and found that the photo-reactivity of doped TiO₂ appeared to be a complex function of the dopant concentration, the distribution of dopants and the electron donor concentration. Obalová *et al.*[23] have reported the enhancement of the photo-catalytic of TiO₂ doped with Ag for the decomposition of nitrous oxide.

Han *et al.*[24] have synthesized titanium nano-sheets with a high percentage of exposed (001) facets which have shown good photo-catalytic properties. Xiang *et al.*[25] have investigated the influences of hydrofluoric acid content on the microstructures and the photo-catalytic activity of TiO₂ nano-sheets. These materials have showed a very good photo-catalytic activity for the degradation of organic dyes. However, the doping and the application of these products for the removal of wide range of chlorinated organic pollutants such as tetrachloroethene (PCE), trichloroethene (TCE) and 1,1,1-trichloroethane (TCA) in aqueous phase under VUV illumination have not been reported. Chlorinated solvents have been commonly used in dry cleaning, degreasing industries as solvents and have

constituted a major public health and environmental concerns[26-28]. Due to their low aqueous solubility, high density and mobility, they are mostly detected in contaminated soil and groundwater. Moreover, they are known to be toxic or carcinogenic and resistant to environmental (chemical, physical and biological) degradation, hence being listed on priority pollutants in the United State Environmental Protection Agency (EPA)[29-31]. Thus, their release into water without appropriated treatment can become a long term pollutant source to environment and human health.

Herein, we investigate the applicability of the synthesized of Cu metal doped titanium nano-sheets in the degradation of tetrachloroethene (PCE), trichloroethene (TCE) and 1,1,1-trichloroethane (TCA) in aqueous phase under VUV irradiation. Since copper salts have been reported to improve electron/hole separation and allow efficient photo-generated electron trapping due to its high electrical conductivity, enormous effort have been made to synthesis various Cu doped TiO$_2$ nano-particles mainly used for hydrogen production[32-38]. Cu-TiO$_2$ has been synthesized by simple hydrothermal method using tetrabutyl titanate and cupric nitrate as the precursors and hydrofluoric acid as a reducing and the morphology controlling agent and was characterized by Brunauer-Emmett-Telle (BET), X-ray photoelectron spectroscopy (XPS), X-ray diffraction (XRD) and Transmission electron microscopy (TEM) analyses. Nitrobenzene was used as a probe to detect the presence of hydroxyl radical ($^\bullet$OH) radicals generated during the photo-degradation process. Based on this study it is anticipated that Cu doping can be used to enhance the photo-catalytic activity of TiO$_2$ nano-sheets, which could be an alternative process in chlorinated solvent remediation in contaminated groundwater.

EXPERIMENTAL

Tetrabutyl-titanate [Ti(OBu)$_4$, 98 %], cupric nitrate [Cu(NO$_3$)$_2$.3H$_2$O], hydrofluoric acid (HF, 45 %), commercial P25 (Degussa), 1,1,1-trichloroethane (TCA, 99 %), tetrachloro-ethene (PCE, 99 %), trichloroethene (TCE, 99 %) hexane (97 %), ethanol (95 %) and nitrobenzene (NB) were purchased from Shanghai Jingchun Reagent Co. Ltd. (Shanghai, China). All chemicals were of analytical grade and used without further purification. Ultrapure water from a Milli-Q water (Classic DI, ELGA, Marlow, U.K.) was used in all experiments.

Catalysts preparation: Cu-TiO$_2$ anatase nano-sheets were synthesized by modification of the hydrothermal method described by Han and co-workers[24]. Briefly, 30 mL Ti(OBu)$_4$, 2 mL HF and 0.08g Cu(NO$_3$)$_2$·3H$_2$O were mixed in a dried Teflon autoclave with a capacity of 50 mL and then kept at 180 °C for 24 h. After cooling to room temperature, the grey precipitate was separated by high-speed centrifugation at 3000 rpm for 15 min, washed with ethanol and double-deionized water for several times to remove impurities and then dried in vacuum at 70 °C for 24 h.

Characterization: The phase structure and phase purity of the synthesized TiO$_2$ were examined by X-ray diffraction (XRD), using a Rigaku D/max 2550VB/PC diffractometer with CuK$_\alpha$ (λ = 0.154 nm) radiation as the incident beam. The surface chemical bonding was characterized by X-ray photoelectron spectroscopy (XPS) measurement using a Thermo Fisher

ESCALAB 250xi with a cylindrical mirror analyzer and an Al K$_\alpha$ radiation at acceleration voltage of 15 kV to examine the atomic composition and oxidation state of each atom on the surface of the synthesized products. The specific surface area and pore size of the materials were obtained by the BET method at liquid nitrogen temperature with a Quantasorb Jr. Instrument (Quantachrome Co. UK). Transmission electron microscopy (TEM) was performed on JEM-1400 electron microscope operated at an accelerating voltage at 80 kV.

Photo-degradation test: The photo-catalytic test was conducted in a 1 L cylindrical glass reactor (containing 3 g of photo-catalyst powder and 20 mg L^{-1} of aqueous solution of pollutant), with a magnetic stirrer located at the base of the reactor to maintain the homogeneity of the solution. A 10 W low-pressure mercury vapor lamp (Guangdong, China) at 185 nm wavelength was used, hereafter, referred to as VUV. The aqueous solution was filled into the reactor and the temperature was kept constant at 20 °C during all experiments with a cooling water jacket using a thermostat circulating water bath (SCIENTZ SDC-6, Zhejiang, China). Aqueous samples were taken at desired time intervals and analyzed immediately. Before illumination, the suspension was stirred for 15 min in dark to reach the adsorption-desorption equilibrium between the pollutant and the photo-catalyst.

Analytical methods: One milliliter was removed from the reactor, periodically throughout the course of the experiment and analyzed after extraction with 1 mL of hexane. The samples were mixed with hexane using a vortex stirrer for 5 min and then allowed to separate by standing for another 5 min. The organic phase was then transferred to a 2 mL GC vial with a plastic dropper and quantified by a gas chromatograph (Agilent 7890A, Palo Alto, CA) equipped with an electron capture detector (ECD), an autosampler (Agilent 7693) and a DB-VRX column (60 m length, 320 μm inner diameter, 1.4 μm thickness). The temperatures of the injector and detector were 240 and 260 °C, respectively and the oven temperature was isothermal at 75 °C. The amount of sample injected was 1 μL with a split ratio of 20:1. The concentration of nitrobenzene was analyzed using the same gas chromatograph (Agilent 7890A, Palo Alto, CA) equipped with an flame ionization detector (FID), an auto-sampler (Agilent 7693) and an HP-5 column (30 m length, 320 μm i.d., 0.25 μm thickness). The temperatures of the injector and detector were 200 and 250 °C, respectively and the oven temperature was constant at 170 °C. The amount of sample injected was 1 μL with a split ratio of 1:1. Chloride (Cl$^-$) was analyzed by ion chromatography (Dionez ICS-I000, Sunnyvale, CA).

RESULTS AND DISCUSSION

Photo-catalytic activity test: The photo-catalytic test of the synthesized TiO$_2$ was carried out by degrading 1,1,1-trichloroethane, trichloroethene and tetrachloroethene in aqueous under VUV (Fig. 1). The degradation patterns of chlorinated solvent pollutants followed the first-order kinetic and the calculated rate constant values are shown in Table-1. Observing the above patterns, the synthesized TiO$_2$ (undoped) and Cu-TiO$_2$ showed approximately the same photocatalytic activity for the degradation of the chlorinated solvent pollutants.

TABLE-1
PARAMETERS OF PCE, TCE AND TCA DEGRADATION IN VUV AND VUV/Cu-TiO$_2$ SYSTEMS

Operational conditions	Quantity (g)	Degradation rate (%)	Degradation rate constant k (min^{-1})	Correlation coefficient R^2
PCE				
VUV alone	-	100	0.5195	0.9973
Commercial P25	3	100	0.1434	0.9807
Synthesized TiO$_2$	3	100	0.5852	0.9956
Cu-TiO$_2$	3	100	0.6819	0.9972
TCE				
VUV alone	-	100	0.1259	0.9951
Commercial P25	3	73.80	0.0374	0.9709
Synthesized TiO$_2$	3	100	0.4075	0.9977
Cu-TiO$_2$	3	100	0.5484	0.9983
TCA				
VUV alone	-	54.86	0.02434	0.9815
Commercial P25	3	21.04	0.00637	0.6402
Synthesized TiO$_2$	3	65.35	0.03011	0.9689
Cu-TiO$_2$	3	67.59	0.03497	0.9699

However, the calculated degradation rate values indicate that the degradations of chlorinated solvent pollutants were fast over Cu-TiO$_2$ according to their degradation rate constants *i.e.* 0.5852 and 0.6819 min^{-1} for tetrachloro-ethene degradation over VUV/synthesized TiO$_2$ and VUV/Cu-TiO$_2$ systems, respectively. The complete degradation (100 %) of tetrachloroethene and trichloroethene occurred within 0.5 h when VUV was applied alone and when VUV was coupled with synthesized TiO$_2$, while, the degradation rate of 1,1,1-trichloroethane was 67 % with the rate constant at 0.03411 min^{-1} over VUV/Cu-TiO$_2$. Following the above observations in the present study, the photo-degradation of chlorinated solvents in aqueous phase is in the following trend: TCA < TCE < PCE, which may be due to the specific electrostatic interactions in each chemical. Furthermore, no peak was observed as by-product according to the GC/MS analysis.
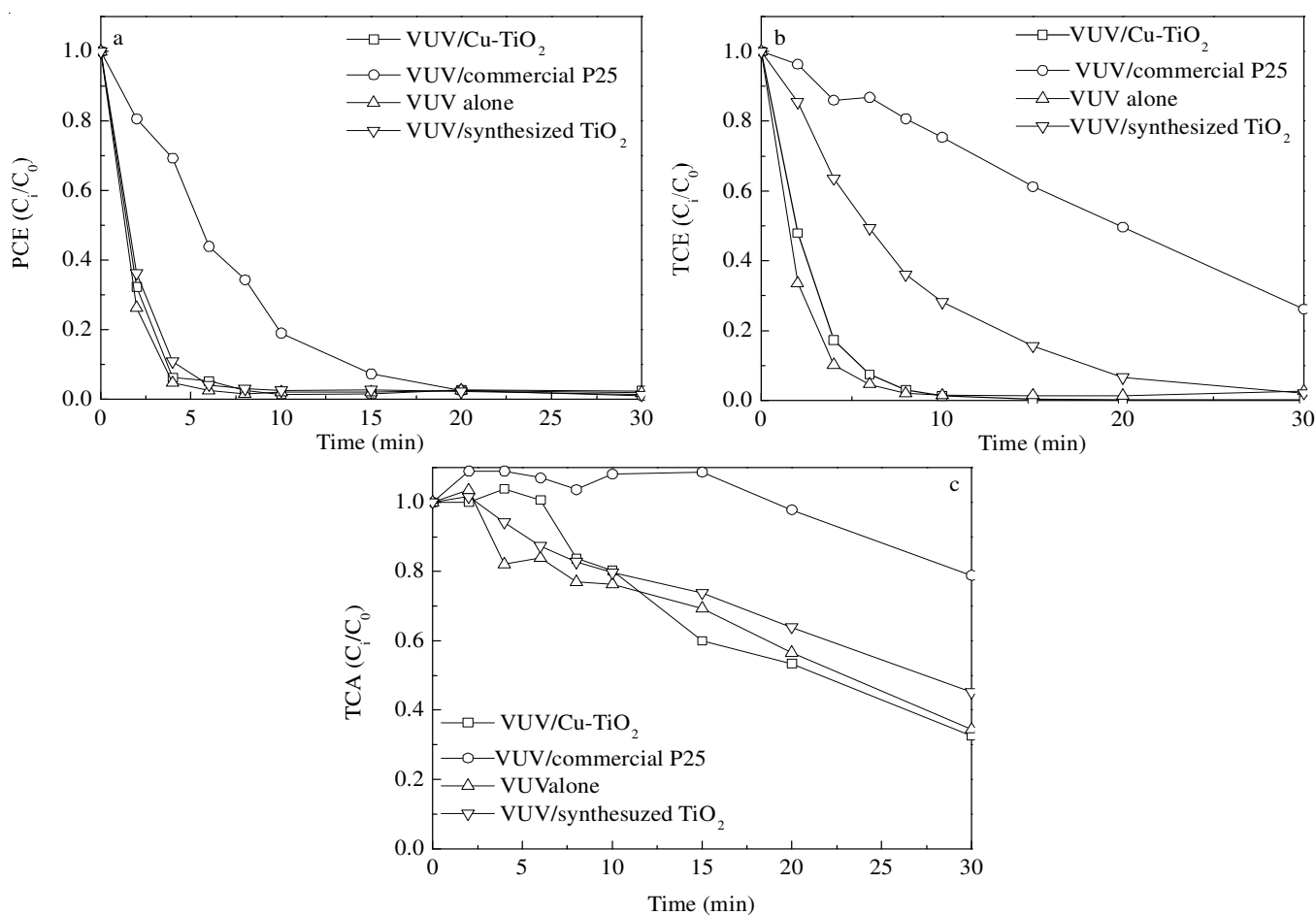

Fig. 1. Photo-degradation performances of (a) tetrachloroethene (PCE), (b) trichloroethene (TCE) and (c) 1,1,1-trichloroethane (TCA)

Dechlorination rate of trichloroethene, *i.e.* moles of Cl⁻ released divided by moles of Cl⁻ in parent trichloroethene, over the synthesized TiO₂, the commercial P25, VUV alone and Cu-TiO₂ are shown in Fig. 2. Compared with the degradation of trichloroethene, the results indicated that the dechlorination rate increased along with the decrease in the concentrations of trichloroethene. Assuming that complete dechlorination of 1 mol of trichloroethene produces 3 mol of Cl⁻, it was estimated that trichloroethene was completely dechlorinated within 20 h over both the synthesized TiO₂ and 0.5 Cu-TiO₂, respectively. Furthermore, no by-products formation was detected according to the GC/MS analysis, suggesting that the pollutants had been completely dechlorinated when VUV was coupled with TiO₂ for the removal of chlorinated solvent pollutants in aqueous phase.

The enhancement of the photo-catalytic activity of the synthesized TiO₂ nano-sheets might be due to the surface ≡Ti–F group on the nano-sheets. It is known that surface ≡Ti–F group can reduce the recombination rate of photo-generated electrons and holes, because it can act as an electron-trapping site to trap the photo-generated electrons by tightly holding trapped electrons due to the strong electronegativity of the fluorine and then transfer them to O₂ adsorbed on the surface of TiO₂[25,39]. After doping with Cu, the photo-catalytic activity was enhanced. The reason may be that, as Cu₂O is a p-type semiconductor and TiO₂ an n-type, when they are coupled together, the photo-generated electrons will have a tendency to transfer from p-Cu₂O to n-TiO₂ and the holes have an opposite transfer because of the inner electric field existed in the p-n junctions between p-Cu₂O and n-TiO₂[32-34]. According to the above photo-catalytic test results, it can be concluded that Cu can be used to enhance the photo-catalytic activity of TiO₂.

It is assumed that chlorinated solvent pollutants were degraded through the oxidation of activated oxygen species generated during reaction in VUV or VUV/TiO₂ systems, especially by hydroxyl radical (•OH) radicals. Therefore, in this study nitrobenzene (NB) was chosen as a probe in order to check the presence of •OH which is known to be responsible of nitrobenzene degradation[40-42]. The photo-degradation test of 0.25 mM of aqueous solution of nitrobenzene and the analysis were conducted at the same conditions as descripted for trichloroethene degradation. The photo-degradation curves are shown in Fig. 3. It is clear that nitrobenzene degradation was better (around 90 %) over VUV/Cu-TiO₂ with the rate constant of 0.03 min⁻¹. The degradation results suggested that the population of •OH generated under VUV alone, VUV/commercial P25 and VUV/synthesized TiO₂ was less than that generated under UV/Cu-TiO₂, thus, the higher photo-degradation rate of nitrobenzene and chlorinated solvent pollutants over the Cu-TiO₂ compared to the commercial P25 and synthesized TiO₂.
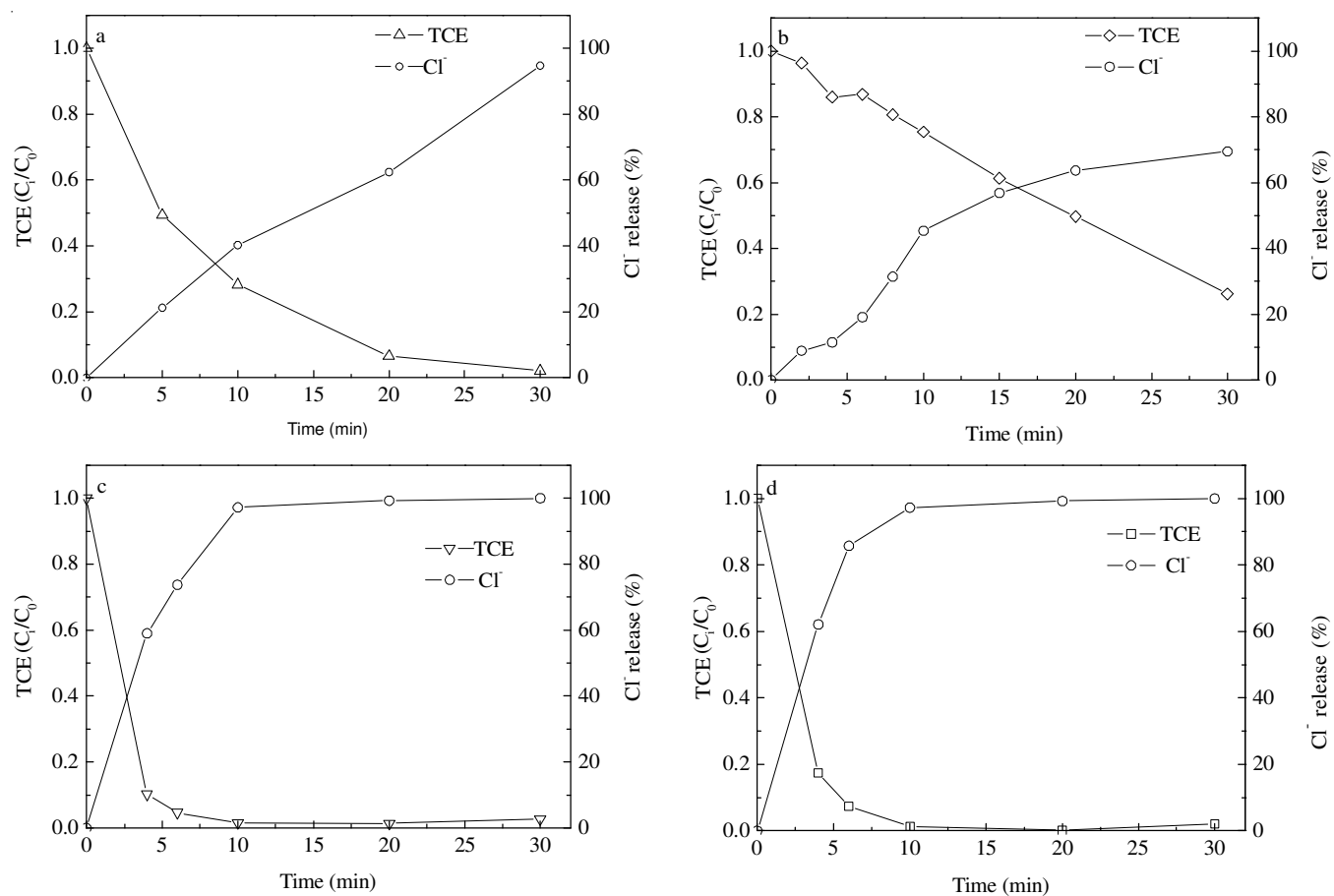

Fig. 2.   Comparison of degradation and dechlorination rate of trichloroethene (TCE) over (a) VUV alone, (b) VUV/commercial P25, (c) VUV/synthesized TiO₂ and (d) VUV/Cu-TiO₂
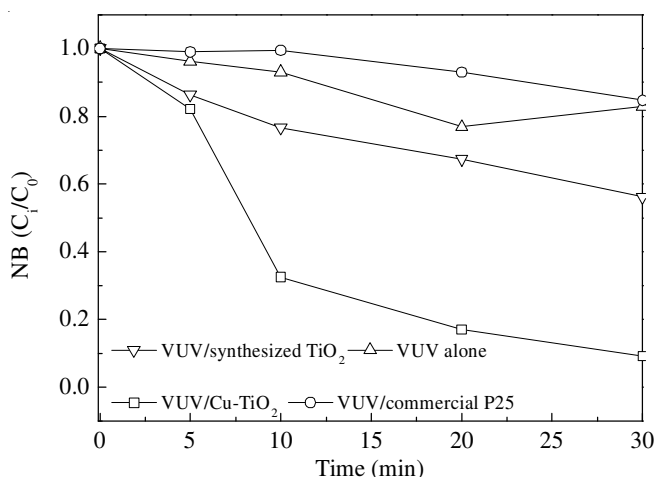
Fig. 3. Photo-degradation of nitrobenzene in various systems

X-ray diffraction: The XRD patterns of the synthesized TiO$_2$ are displayed in Fig. 4. In both cases, the synthesized products exhibited strong diffraction peak that is proved in their high crystallinity[43]. In line a, the diffraction peak of the synthesized TiO$_2$ appeared at 2θ of 25.3°, 37.8°, 48.1°, 55.1°, 62.7°, 70.3° and 75.1° can be indexed as pure TiO$_2$ anatase phase (JCPDS No. 21-1272) which is conformed to the literatures[24,25]. Line b is the XRD pattern of Cu-TiO$_2$. As it is shown, no diffraction peak of Cu is observed that is might be due to the low content of Cu and its high dispersion degree on the surface of the product[44]. The parameter values in Table-2 showed that the doping of Cu on TiO$_2$ nano-sheets can change the physico-chemical properties on the surface of TiO$_2$, *i.e.*, the increase of the specific surface area and the decrease of crystalline size after the doping.
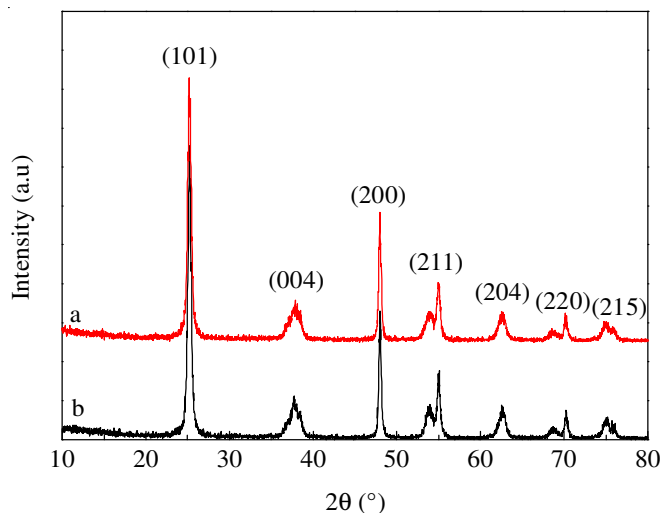

Fig. 4. XRD patterns of the synthesized products

The crystallinity and crystal phase are important parameters which influence photo-catalyst behavior. Highly crystalline TiO$_2$ structure is required to achieve high photo-catalytic activity and previous studies have demonstrated that surface fluorination of TiO$_2$ can be used as a new method of surface modification on crystallite size and phase[24,25]. From the above observations, Cu doping did not change the crystalline phase of the synthesized product.

TABLE-2
EFFECTS OF CU CONTENT ON PHYSICO-CHEMICAL PROPERTIES OF THE SYNTHESIZED PRODUCTS

Samples	Surface area (m^2 g^{-1})	Pore diameter (nm)	Pore volume (cm^3 g^{-1})
Synthesized TiO$_2$	90.3	14.1	0.3
Cu-TiO$_2$	98.5	13.1	0.3

TEM imaging: Transmission electron microscopy images, shown in Fig. 5, indicated that the synthesized TiO$_2$ consisted of well-defined sheet-shaped structures having a rectangular outline with approximately a thickness of 4 nm and are differed from their length and width. From the TEM observations, the synthesized TiO$_2$ nano-sheets product has side length of about 50 nm and width of 33 nm (Fig. 5a), while, the Cu-TiO$_2$ product has the side length of 61 nm and width of 37 nm (Fig. 5b). These images confirmed that HF can be used to synthesized high surface area of the product and Cu can influence the growth of the nano-products, as reported in other literatures[34-36,45].
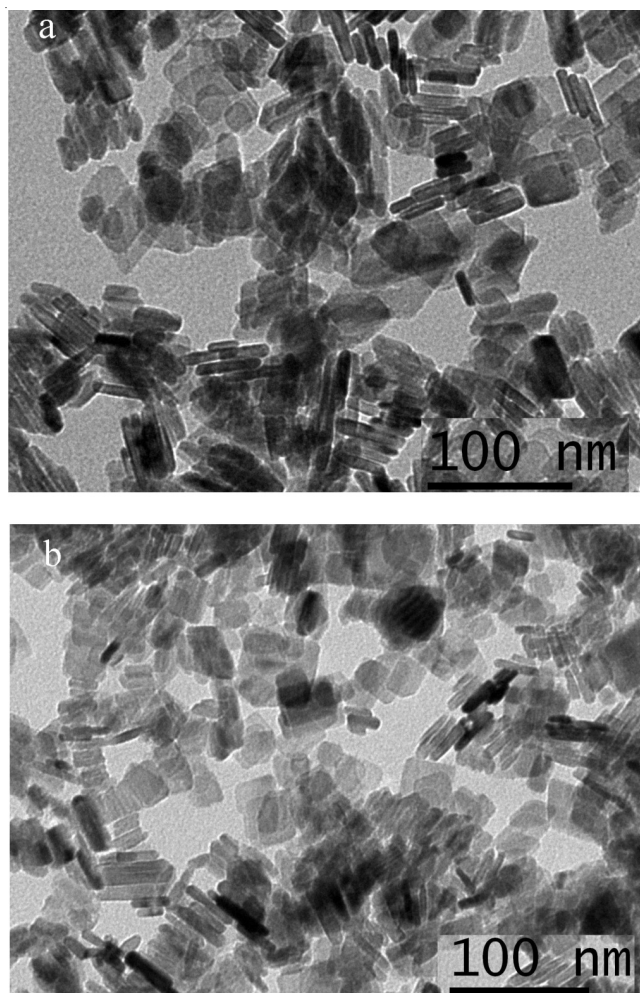

Fig. 5. TEM images of the synthesized products (a) synthesized TiO$_2$ and (b) Cu-TiO$_2$

As in heterogeneous photo-catalysis, oxidation reactions usually take place on the surface of TiO$_2$. The chlorinated solvent pollutants are adsorbed on the surface of nano-sheets and later, are readily degraded due to the uniform illumination on the surface of TiO$_2$.

XPS characterization: In order to investigate the photo-catalytic activity performance of the synthesized products, we further examined the change in surface chemical bonding of the TiO₂ nano-sheets by XPS. The XPS survey spectra of the undoped synthesized TiO₂ and Cu-TiO₂ are displayed in Fig. 6.
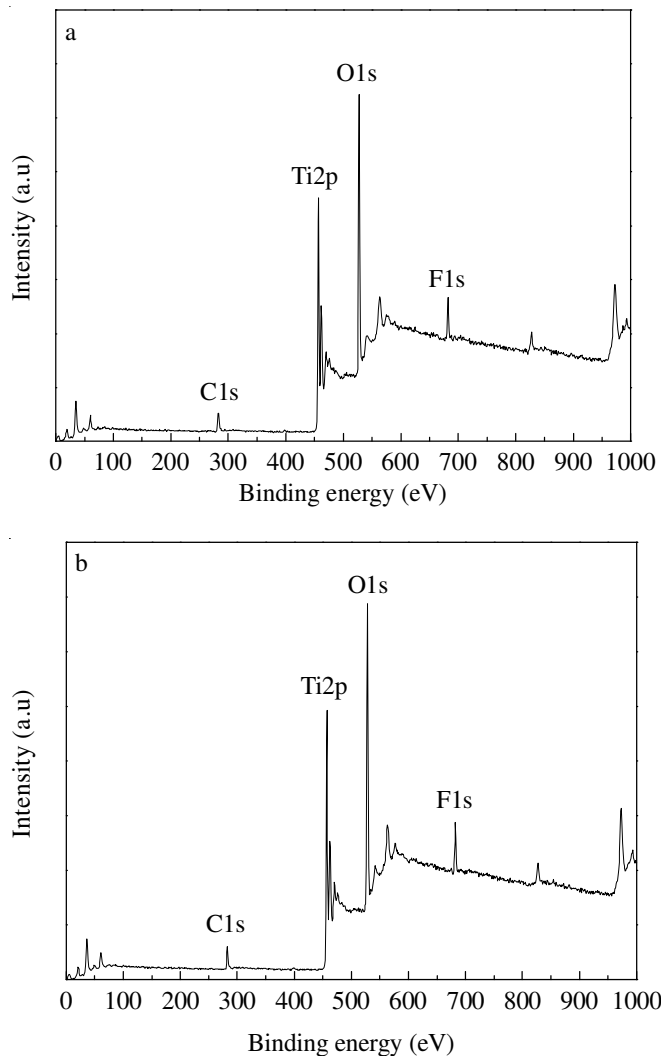

Fig. 6.   XPS survey spectra of the synthesized products (a) synthesized TiO₂ and (b) Cu-TiO₂

The respective photo-electron peaks binding energies of F, Ti, O, Cu and C elements were found to be 682.6 eV (F1s), 462.2 eV (Ti2p), 531.7 eV (O1s) and 284.8 eV (C1s). As predicted, the peak of Cu is not observed in the survey spectra (Fig. 6a) for the Cu-TiO₂ which is in agreement with the XRD analysis. From these binding energies, we can deduce that F, Ti, O and C atoms have a similar bonding environment after Cu doping. The XPS scan spectra of Cu2p is displayed in Fig. 7. As it is shown, the synthesized Cu-TiO₂ exhibited only two typical Cu 2p3/2 and Cu 2p1/2 peaks at 930.7 and 950.8 eV, respectively, which were attributed to Cu⁺ oxidation of Cu₂O. Therefore, no shake-up peak was observed[35,46]. It has also been reported that Cu₂O is more negative than CuO and Cu₂O/TiO₂ photo-catalysts, exhibiting a higher photo-catalytic activity compared to CuO/TiO₂[32,35,46]. The scan spectra of O1s from undoped TiO₂ and Cu-TiO₂ are shown in Fig. 8. According to

the observed results, the main peak appeared in above spectrum at the same position (531.71 eV) is attributed to OII onto surface adsorbed oxygen (O²⁻ or O⁻), •OH groups and oxygen vacancies.
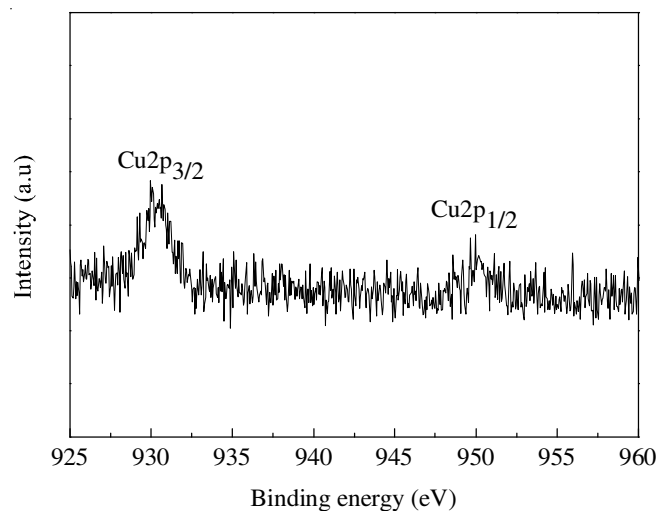

Fig. 7. Cu₂p XPS scan spectrum of Cu-TiO₂

This analysis may explain the relatively high photo-catalytic activity of TiO₂ for the degradation of chlorinated solvent pollutants and nitrobenzene[47,48].
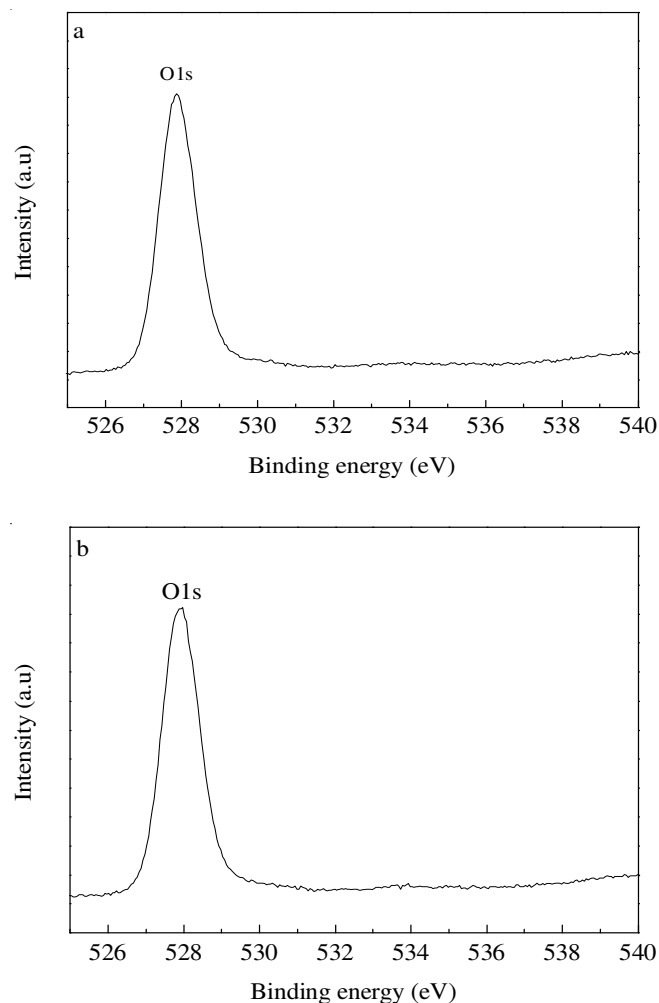

Fig. 8. O1s XPS scan spectra. (a) TiO₂ and (b) Cu-TiO₂

Carbon peak is attributed to the residual carbon from the sample and adventitious hydrocarbon from the XPS instrument itself while, the detected fluorine species identified in Fig. 6 can be attributed to the ≡Ti-F surface bonds formed by ligand exchange reaction between F⁻ and the surface hydroxyl group on the surface of TiO_2[25,46,49]. According to the XPS analysis, Cu doping did not modified the surface state of the synthesized products, probably due to the synthesis method used in our experiment. Moreover, previous studies claimed that the addition of few Cu promoted charge separation and inhibited photo-excited electrons and holes recombination, therefore enhancing photo-catalytic activity of TiO_2[35].

Conclusion

Copper metal doped TiO_2 anatase nano-sheets have been synthesized by a simple hydrothermal method and their photo-catalytic activity have been successfully tested for the degradation of three chlorinated solvent pollutants such as 1,1,1-trichloroethane, trichloroethene and tetrachloroethene in aqueous solution under VUV illumination. The photo-degradation rate of the tested chlorinated solvent pollutants was higher over the Cu-TiO₂ nano-sheets. The degradation rate, which was in the following trend TCA < TCE < PCE, suggested that TCA was the most recalcitrant chlorinated solvent pollutant. Moreover, the degradation result of nitrobenzene, which was better over VUV/Cu-TiO₂, indicated that •OH was generated during the degradation process. The characterization methods using XRD, BET and TEM revealed that the synthesized product which consisted in well-defined sheet-shaped structures, exhibited high crystallinity and high surface area. The XPS analysis has shown that the synthesized product possessed identical elements state (Ti, O, C and F) and surface bonding environment after Cu doping. Cu was in form of Cu₂O corresponding to Cu⁺ oxidation state on the surface of the synthesized TiO₂ nano-sheets. In conclusion, the experimental results suggested that the use of Cu could enhance the photo-catalytic activity of TiO₂ for wide application in chlorinated solvent remediation in contaminated groundwater.

REFERENCES

1. S. Jõks, D. Klauson, M. Krichevskaya, S. Preis, F. Qi, A. Weber, A. Moiseev and J. Deubener, *Appl. Catal. B*, **111-112**, 1 (2012).
2. A. Fujishima and K. Honda, *Nature*, **238**, 37 (1972).
3. A. Kimoto and S. Shimada, *Sens. Actuators A*, **175**, 150 (2012).
4. A. Kitada, G. Hasegawa, Y. Kobayashi, K. Kanamori, K. Nakanishi and H. Kageyama, *J. Am. Chem. Soc.*, **134**, 10894 (2012).
5. L. Kumaresan, M. Mahalakshmi, M. Palanichamy and V. Murugesan, *Ind. Eng. Chem. Res.*, **49**, 1480 (2010).
6. S. Suthersan and J. Horst, *Ground Water Monit. Remediat.*, **28**, 153 (2008).
7. H. Chen, C.E. Nanayakkara and V.H. Grassian, *Chem. Rev.*, **112**, 5919 (2012).
8. X. Chen and S.S. Mao, *Chem. Rev.*, **107**, 2891 (2007).
9. Y. Du and J. Rabani, *J. Phys. Chem. B*, **107**, 11970 (2003).
10. S.Y. Chae, M.K. Park, S.K. Lee, T.Y. Kim, S.K. Kim and W.I. Lee, *Chem. Mater.*, **15**, 3326 (2003).
11. Y. Bessekhouad, D. Robert, J.V. Weber and N. Chaoui, *J. Photochem. Photobiol. Chem.*, **167**, 49 (2004).
12. Y. Ishibai, J. Sato, T. Nishikawa and S. Miyagishi, *Appl. Catal. B*, **79**, 117 (2008).
13. S.K. Choi, S. Kim, S.K. Lim and H. Park, *J. Phys. Chem. C*, **114**, 16475 (2010).
14. C. Miranda, H. Mansilla, J. Yáñez, S. Obregón and G. Colón, *J. Photochem. Photobiol. Chem.*, **253**, 16 (2013).
15. X. Zou, J. Liu, J. Su, F. Zuo, J. Chen and P. Feng, *Chem. Eur. J.*, **19**, 2866 (2013).
16. Z. Li, B. Hou, Y. Xu, D. Wu and Y. Sun, *J. Colloid Interf. Sci.*, **288**, 149 (2005).
17. M.V. Dozzi, S. Livraghi, E. Giamello and E. Selli, *Photochem. Photobiol. Sci.*, **10**, 343 (2011).
18. M.A. Fox and M.T. Dulay, *Chem. Rev.*, **93**, 341 (1993).
19. M.R. Hoffmann, S.T. Martin, W. Choi and D.W. Bahnemann, *Chem. Rev.*, **95**, 69 (1995).
20. A.L. Linsebigler, G. Lu and J.T. Yates, *Chem. Rev.*, **95**, 735 (1995).
21. F. Dong, H. Wang and Z. Wu, *J. Phys. Chem. C*, **113**, 16717 (2009).
22. W. Choi, A. Termin and M.R. Hoffmann, *J. Phys. Chem.*, **98**, 13669 (1994).
23. L. Obalová, M. Reli, J. Lang, V. Matejka, J. Kukutschová, Z. Lacný and K. Kočí, *Catal. Today*, **209**, 170 (2013).
24. X. Han, Q. Kuang, M. Jin, Z. Xie and L. Zheng, *J. Am. Chem. Soc.*, **131**, 3152 (2009).
25. Q. Xiang, K. Lv and J. Yu, *Appl. Catal. B*, **96**, 557 (2010).
26. R.E. Doherty, *Env. Forensics.*, **1**, 83 (2000).
27. S. Tabrez and M. Ahmad, *Int. J. Hyg. Environ. Health*, **215**, 333 (2012).
28. M.O. Rivett, D.N. Lerner and J.W. Lloyd, *Water Environ. J.*, **4**, 242 (1990).
29. K. Wilson, G. Sewell, J.A. Kean and K. Vangelas, *Rem. J.*, **17**, 39 (2007).
30. J.C. Chambon, P.L. Bjerg, C. Scheutz, J. Bælum, R. Jakobsen and P.J. Binning, *Biotechnol. Bioeng.*, **110**, 1 (2013).
31. C. Lu, P.L. Bjerg, F. Zhang and M.M. Broholm, *Chemosphere*, **83**, 1467 (2011).
32. J. Yu, Y. Hai and M. Jaroniec, *J. Colloid Interface Sci.*, **357**, 223 (2011).
33. H. Irie, K. Kamiya, T. Shibanuma, S. Miura, D.A. Tryk, T. Yokoyama and K. Hashimoto, *J. Phys. Chem. C*, **113**, 10761 (2009).
34. T. Nogawa, T. Isobe, S. Matsushita and A. Nakajima, *Mater. Lett.*, **82**, 174 (2012).
35. L. Li, L. Xu, W. Shi and J. Guan, *Int. J. Hydrogen Energy*, **38**, 816 (2013).
36. J. Araña, A. Peña Alonso, J.M. Doña Rodríguez, J.A. Herrera Melián, O. González Díaz and J. Pérez Peña, *Appl. Catal. B*, **78**, 355 (2008).
37. S.-K. Li, X. Guo, Y. Wang, F.-Z. Huang, Y.-H. Shen, X.-M. Wang and A.-J. Xie, *Dalton Trans.*, **40**, 6745 (2011).
38. O. Baghriche, S. Rtimi, C. Pulgarin, R. Sanjines and J. Kiwi, *J. Photochem. Photobiol. Chem.*, **251**, 50 (2013).
39. K. Lv, B. Cheng, J. Yu and G. Liu, *Phys. Chem. Chem. Phys.*, **14**, 5349 (2012).
40. T.-J. Whang, M.-T. Hsieh, T.-E. Shi and C.-H. Kuei, *Int. J. Photoenergy*, **2012**, 1 (2012).
41. B. Legube and N. Karpel Vel Leitner, *Catal. Today*, **53**, 61 (1999).
42. X.-Z. Shen, Z.-C. Liu, S.-M. Xie and J. Guo, *J. Hazard. Mater.*, **162**, 1193 (2009).
43. G. Wang, L. Xu, J. Zhang, T. Yin and D. Han, *Int. J. Photoenergy*, **Article ID 265760** (2012).
44. L.S. Yoong, F.K. Chong and B.K. Dutta, *Energy*, **34**, 1652 (2009).
45. W. Jiao, L. Wang, G. Liu, G.Q. Lu and H.-M. Cheng, *ACS Catal.*, **2**, 1854 (2012).
46. Y.H. Kim, D.K. Lee, H.G. Cha, C.W. Kim, Y.C. Kang and Y.S. Kang, *J. Phys. Chem. B*, **110**, 24923 (2006).
47. W.Y. Hernández, M.A. Centeno, S. Ivanova, P. Eloy, E.M. Gaigneaux and J.A. Odriozola, *Appl. Catal. B*, **123-124**, 27 (2012).
48. M.M. Rashid and C. Sato, *Water Air Soil Pollut.*, **216**, 429 (2011).
49. Y. Wang, H. Zhang, Y. Han, P. Liu, X. Yao and H. Zhao, *Chem. Commun.*, **47**, 2829 (2011).